

Evaluation of the rotenone-induced activation of the Nrf2 pathway in a neuronal model derived from human induced pluripotent stem cells

Dimitra Zagoura, David Canovas-Jorda, Francesca Pistollato, Susanne Bremer-Hoffmann,
Anna Bal-Price*

Directorate F – Health, Consumers and Reference Materials, Joint Research Centre, Ispra, Italy

ARTICLE INFO

Article history:

Received 3 June 2016

Received in revised form

25 August 2016

Accepted 6 September 2016

Available online xxxx

Keywords:

Human induced pluripotent stem cells

Neuronal/glial cultures

Nrf2 pathway

Rotenone

ABSTRACT

Human induced pluripotent stem cells (hiPSCs) are considered as a powerful tool for drug and chemical screening and development of new *in vitro* testing strategies in the field of toxicology, including neurotoxicity evaluation. These cells are able to expand and efficiently differentiate into different types of neuronal and glial cells as well as peripheral neurons. These human cells-based neuronal models serve as test systems for mechanistic studies on different pathways involved in neurotoxicity.

One of the well-known mechanisms that are activated by chemically-induced oxidative stress is the Nrf2 signaling pathway. Therefore, in the current study, we evaluated whether Nrf2 signaling machinery is expressed in human induced pluripotent stem cells (hiPSCs)-derived mixed neuronal/glial culture and if so whether it becomes activated by rotenone-induced oxidative stress mediated by complex I inhibition of mitochondrial respiration.

Rotenone was found to induce the activation of Nrf2 signaling particularly at the highest tested concentration (100 nM), as shown by Nrf2 nuclear translocation and the up-regulation of the Nrf2-downstream antioxidant enzymes, NQO1 and SRXN1. Interestingly, exposure to rotenone also increased the number of astroglial cells in which Nrf2 activation may play an important role in neuroprotection. Moreover, rotenone caused cell death of dopaminergic neurons since a decreased percentage of tyrosine hydroxylase (TH⁺) cells was observed. The obtained results suggest that hiPSC-derived mixed neuronal/glial culture could be a valuable *in vitro* human model for the establishment of neuronal specific assays in order to link Nrf2 pathway activation (biomarker of oxidative stress) with additional neuronal specific readouts that could be applied to *in vitro* neurotoxicity evaluation.

© 2016 The Authors. Published by Elsevier Ltd. This is an open access article under the CC BY-NC-ND license (<http://creativecommons.org/licenses/by-nc-nd/4.0/>).

1. Introduction

Human induced pluripotent stem cells (hiPSCs) represent unique tools for toxicity screening and improved mechanistic understanding of chemically-induced adverse effects (Hou et al., 2013; Kumar et al., 2012; Yap et al., 2015). This is in line with the report “Toxicity Testing in the twenty-first Century” released in 2007 by the National Research Council of the United States that encourages the use of human cell-based models for *in vitro* toxicity testing (NRC, 2007). Opposite to human cell lines derived from carcinoma tissues (e.g. neuroblastoma cell lines), which do not possess normal cell physiology, hiPSCs have been identified as a potential source of various cell types for toxicity testing (Hou et al., 2013). HiPSCs share similar characteristics with human embryonic stem cells (hESCs) (Krueger et al., 2010; Pistollato et al., 2012), i.e. are characterized by unlimited self-renewal and capacity to

Abbreviations: AOPs, Adverse Outcome Pathways; ARE, Antioxidant-Responsive-Element; GABA, Gamma-Aminobutyric Acid; GABRA1, Gamma-Aminobutyric Acid Type A Receptor Alpha1 Subunit; GABRA3, Gamma-Aminobutyric Acid Type A Receptor Alpha3 Subunit; GAP43, Growth Associated Protein 43; GAPDH, Glyceraldehyde 3-phosphate dehydrogenase; GFAP, Glial Fibrillary Acidic Protein; GSR, Glutathione Reductase; GRIA1, Glutamate Ionotropic Receptor AMPA Type Subunit 1; HCl, High Content Imaging; hESCs, Human Embryonic Stem Cells; hiPSCs, Human Induced Pluripotent Stem Cells; HMOX1, Heme Oxygenase-1; IATA, Integrated Approaches to Testing and Assessment; Keap1, Kelch-like ECH-Associated Protein 1; MAP2, Microtubule-Associated Protein 2; MEA, Multi Electrode Array; MFR, Mean Firing Rate; NF200, Neurofilament 200; NQO1, NAD(P)H Quinone Oxidoreductase 1; NR4A2, Nuclear Receptor Subfamily 4 Group A Member 2; Nrf2, Nuclear Factor (erythroid-derived 2)-like 2; NSCs, Neural Stem Cells; Pax6, Paired Box 6; PSCs, Pluripotent Stem Cells; SRXN1, Sulfiredoxin1; TH, Tyrosine Hydroxylase; VGlut1, Vesicular Glutamate Transporter 1.

* Corresponding author. European Commission JRC, Directorate F – Health, Consumers and Reference Materials, Via E. Fermi 2749 TP 580, I-21027 Ispra, VA, Italy.

E-mail address: anna.price@ec.europa.eu (A. Bal-Price).

<http://dx.doi.org/10.1016/j.neuint.2016.09.004>

0197-0186/© 2016 The Authors. Published by Elsevier Ltd. This is an open access article under the CC BY-NC-ND license (<http://creativecommons.org/licenses/by-nc-nd/4.0/>).

generate different human tissue-specific somatic cells (Avior et al., 2016; Robinton and Daley, 2012), including neurons and glial cells. Moreover, these stem cell-based systems offer an innovative alternative for obtaining a large number of human cells, serving as a valuable tool for the development of *in vitro* models for toxicity testing (Avior et al., 2016), often applicable for high throughput screening (HTS) (Desbordes and Studer, 2013). Therefore, hiPSC-derived *in vitro* models have a great potential to improve the efficacy of drug discovery as well as human risk assessment. However, before this can be achieved, quality control criteria, specific for the morphological and functional characterization of hiPSC-derivatives are required to ensure reproducibility and reliability of data produced for regulatory toxicology use (Pistollato et al., 2012). For instance, the expression of Paired Box 6 (Pax6) and Nestin will be important to characterize neuroectodermal commitment, analysis of MAP2, synaptophysin (SYN) and microtubule-associated protein tau (MAPT) to confirm neuronal differentiation, while expression of GFAP is essential to determine the presence of astrocytes.

Oxidative stress is one of the non-cell specific cellular responses (including neurons and astrocytes) determined at early stages of toxicity and induced by many different classes of chemicals. Key regulators of the Antioxidant-Response-Element-(ARE)-driven cellular defense mechanisms against oxidative stress is the Nuclear factor (erythroid-derived 2)-like 2 (Nrf2), which has a cytoprotective role in several diseases (Ramsey et al., 2007). Upon activation, Nrf2 binds to the promoter regions of several genes, inducing the expression of enzymes that support detoxification processes that take place in many neurodegenerative diseases (Ramsey et al., 2007). Moreover, Nrf2 plays a central role in the regulation of anti-oxidant defense mechanisms in many cell types (if not all). Therefore, analysis of Nrf2 signaling activation could serve as a base for the establishment of a horizontal assay, relevant to different organ toxicity, permitting assessment of oxidative stress induction. Accordingly, several studies have shown that Nrf2 up-regulation is a biomarker of an increased production of reactive oxygen species (ROS) that contribute to various neurodegenerative diseases, including Parkinson disease (Ramsey et al., 2007; Tufekci et al., 2011).

In the current study, we exposed hiPSC-derived mixed neuronal and glial cultures to rotenone, an inhibitor of mitochondrial respiratory complex I that is linked to Parkinson disease, as shown in animal models upon chronic exposure to rotenone at low doses (Cannon et al., 2009; Sherer et al., 2003; Tanner et al., 2011). In particular, in a rodent model of Parkinson disease rotenone was found to induce irreversible, selective dopaminergic neuronal cell death and formation of Lewy body-like cytoplasmic inclusions (Cannon et al., 2009; Sherer et al., 2003; Tanner et al., 2011).

In this study we assessed the activation of Keap1-Nrf2-ARE pathway in a hiPSC-derived neuronal culture upon acute (24 h) treatment with non-cytotoxic concentrations of rotenone (i.e., 1–10–100 nM), and detected its possible effects on neuronal and glial cell markers. The evaluation of the expression of the Nrf2 pathway in human stem cell-derived neuronal/glial models could serve for future *in vitro* screening and prioritization for further testing of potential neurotoxic compounds that act through Nrf2 signaling activation and induction of oxidative stress.

2. Materials and methods

2.1. Human iPSC culture, expansion and treatments

IMR90-hiPSCs were kindly provided by Dr. Marc Peschanski (I-stem, France). IMR90 fibroblast cell line was established on 07/07/1975 using explants of minced lung tissue obtained from a clinically normal 16 week old fetus and they exhibit a normal female

karyotype (46, XX) http://ccr.coriell.org/Sections/Search/Sample_Detail.aspx?Ref=I90-52&PgId=166.

IMR90 fibroblasts were reprogrammed into hiPSCs at I-Stem by viral transduction of 2 transcription factors (Oct4 and Sox2) by using the pMIG vectors (Addgene).

hiPSCs were cultured, under feeder-free conditions, on matrigel™ hESC-qualified matrix (Corning) pre-coated Petri-dishes in the presence of mTeSR™1 medium containing mTeSR™1 5X supplements (Stem Cell Technologies) prepared following manufacturer's instructions. HiPSC colonies were passaged by microdissection using a 30G needle. Cells were treated with 1, 10, 100 nM rotenone (Sigma-Aldrich, dissolved in DMSO) for 24 h, accounting for solvent control analysis. A 24 h treatment with 10 μM and 100 μM hydrogen peroxide (H₂O₂, Sigma-Aldrich) was used as a positive control for induction of oxidative stress and activation of the Nrf2 pathway.

Additionally, human neurons derived from adult brain tissue (InnoProt, reference number P10151), and rat embryonic cortical neurons (Sigma-Aldrich, embryonic day 18, reference number R882N), cultured as described by the manufacturers, were used as benchmarks of neuronal cell model performance.

2.2. iPSC-derived neural stem cell expansion and neuronal differentiation protocols

IMR90 cells were differentiated toward neurons and glia following a protocol described in <https://ecvam-dbalm.jrc.ec.europa.eu/beta/index.cfm/methodsAndProtocols/index>, which is a modified version of the method described by Pistollato (Pistollato et al., 2014). Briefly, IMR90-derived colonies cultured on matrigel™ hESC-qualified matrix (Corning) coated dishes were manually microdissected into 200 μm × 200 μm fragments using a 30G needle. For the generation of embryoid bodies (EBs), fragments were transferred into a low attachment Petri-dish (Greiner) and cultures in EB medium ([Supplementary Table 1](#)). After 48 h, generated EBs were plated on laminin (Sigma-Aldrich)-coated dishes and cultured in neuroepithelial induction (NRI) medium ([Supplementary Table 2](#)) for further 7 days. On day 8, neuroepithelial aggregates (rosettes) were visible and were cut in fragments using a 30G needle under a phase contrast microscope. Then, rosettes were spun down, resuspended in 1 ml of phosphate-buffered saline (PBS, 1X) and partially dissociated using a p1000 tip. Finally, dissociated rosettes were plated on laminin-coated dishes and cultured in the presence of neural differentiation (ND) medium for 3 weeks ([Supplementary Table 3](#)).

Moreover, a protocol for the expansion of rosette-derived neural stem cells (NSCs) was developed, as described in <https://ecvam-dbalm.jrc.ec.europa.eu/beta/index.cfm/methodsAndProtocols/index>. Briefly, rosette-derived NSCs were passaged by enzymatic dissociation using 0.05% Trypsin-EDTA (ThermoFisher, 15400-054), and replated on matrigel® basement membrane matrix (Corning) coated dishes in the presence of neural induction (NI) medium ([Supplementary Table 4](#)) (50,000 cells/cm²). NI medium was refreshed every other day. At early passages (1–4), a cell plating density of about 75,000 cells/cm² was applied to improve cell viability after passaging. NSCs were cryopreserved in a freezing solution formulated as follows: 50 mg/ml BSA diluted in complete mTeSR-1 Basal Medium (with mTeSR-1 supplements) (50%), complete NI medium (40%) and DMSO (10%). NSCs were differentiated into neuronal mixed cultures using ND medium as described above.

2.3. Immunocytochemistry

About 6000–7000 cells/well in 96 well plates were plated and differentiated for 21 days. On day 21, cells were treated with either

rotenone or H₂O₂ as described above, and after 24 h cells were fixed with cold 4% paraformaldehyde, washed in PBS 1X, permeabilized in PBS 1X containing 0.1% Triton-X-100 and 3% bovine serum albumin (BSA) for 15 min at room temperature, and further incubated with 3% BSA/1X PBS (blocking solution) to prevent nonspecific binding of the antibodies. The cells were then incubated with primary antibodies as follows: neurofilament 200 (NF200, rabbit, 1:1000, Sigma-Aldrich), glial fibrillary acidic protein (GFAP, mouse, 1:500, Merck-Millipore), microtubule-associated protein-2 (MAP2, mouse, 1:500, Sigma-Aldrich), synaptophysin (SYN, rabbit, 1:200, Abcam), Nrf2 (rabbit), Keap1 (rabbit), sulfiredoxin1 (SRXN1, goat), NAD(P)H quinone oxidoreductase 1 (NQO1, goat) (all 1:200, Abcam), nestin (rabbit, 1:200, Sigma-Aldrich), tyrosine hydroxylase (TH, rabbit, 1:200, Millipore), gamma-aminobutyric acid (GABA, mouse, 1:100, Sigma-Aldrich), vesicular glutamate transporter 1 (VGAT1, rabbit, 1:500, Abcam) in blocking solution overnight at 4 °C. The cells were washed with PBS and further incubated with fluorochrome-conjugated secondary antibodies (1:1000, Invitrogen). Nuclei were counterstained with DAPI dye (0.3 μM, Sigma-Aldrich). Quantification of mean fluorescence intensity and of the relative percentages of cell types was performed using two specific ArrayScan algorithms: Cytotoxicity V.4 and NucTrans V.4 bio-applications. Both the applications apply a specific nuclear mask around the DAPI staining defined according to nuclear morphology, discarding invalid nuclei (i.e., nuclei that were pyknotic, bright and/or dense clumps of cells) and, on the valid nuclei (i.e., homogenous round-shaped nuclei, indicative of live cells) an additional cell body shape mask was applied according to the type of antibody/antigen staining, as already described (O'Brien et al., 2006). The NucTrans V.4 algorithm calculates the level of fluorescence intensity both in the nucleus and the cytoplasm, applying respectively a circular mask (for nuclear signal) and a ring shape mask (for cytoplasmic signal). Secondary antibody incubation alone was used to determine the intensity level of fluorescent background that was subtracted. The ArrayScan™ XTI High Content Platform was set up to take a minimum of 20 pictures/well. Each staining was done on 7–8 internal replicates for each condition.

2.4. Electrophysiological measurements

Dissociated rosette-like structures (differentiation day 7) or NSCs derived from rosettes were plated on Multielectrode arrays (MEAs) (1×10^5 cells/MEA chip) containing complete ND medium and differentiated for 3 weeks as described above. Additionally, human neurons derived from adult brain tissue (InnoProt, Ref. number P10151), and rat embryonic cortical neurons (Sigma-Aldrich, embryonic day 18, Ref. number R882N) were cultured respectively for 2 and 3 weeks directly on MEA chips to allow neuronal network formation and maturation. Electrical activity of these cultures was evaluated in comparison to the hiPSC-derived neuronal model. At the end of differentiation, the mixed hiPSC-derived neuronal cultures were exposed to 1–10–100 nM rotenone for 24 h, on MEA plates which were sealed with a semi-permeable membrane (standard MEAs) in a laminar flow hood to keep the cultures sterile for repeated measurements. Each chip (single well) contains 60 microelectrodes, aligned in an 8 × 8 square grid, with the four corners missing. One of the electrodes can be replaced by one ground reference, allowing recording from the remaining 59 electrodes. The mean firing rate (MFR, number of spikes/min) was recorded prior to the addition of rotenone (which represents the control value) and, after 24 h, MEA recording was repeated and data were normalized to control (Ctr). All data represent the average of at least $n = 3$ biological replicates. The measurements were performed with a MEA1060-Inv-BC-amplifier with integrated temperature process control adjusted to 37 °C and

5%CO₂ and data were recorded with MC Rack software (Multi-channel systems). Peaks from MEA raw data were detected using threshold limit of -4.7σ , where σ represents the standard deviation of the basal noise. From each MEA, the number of spikes/min and bursts/30 min were calculated (a burst was considered as a train of at least 2–5 action potentials occurring max every 100 msec). Spike number data were normalized with respect to baseline activity for each MEA separately. Post-recording data were processed with NeuroExplorer (NexTechnologies) and Excel (Microsoft).

2.5. Quantitative real-time PCR (qPCR) analyses

Analysis of gene expression by qPCR was performed on differentiated and rotenone-treated (i.e., 1–10–100 nM) and untreated (control) cells. RNA was isolated using the RNAqueous®-Micro Kit (ThermoFisher) according to manufacturer's instructions, and 500 ng of total RNA was reverse transcribed using the High Capacity cDNA Reverse Transcription Kit (as directed, ThermoFisher). qPCR reactions were run in duplicate using TaqMan® Gene Expression Master Mix (ThermoFisher) and the following TaqMan gene expression assays (all from ThermoFisher): GFAP (Hs00909233_m1), MAP2 (Hs00258900_m1), NQO1 (Hs02512143_s1), SRXN1 (Hs00607800_m1), HMOX1 (Hs0110250_m1), GSR (Hs00167317_m1), PAX6 (Hs01088112_m1), NES (Hs00707120_s1), GRIA1 (Hs00181348_m1), GAP43 (Hs00967138_m1), GABRA3 (Hs00968132_m1), GABRA1 (Hs00168058_m1), NR4A2 (Hs00428691_m1), TH (Hs00165941_m1), GAPDH (Hs02758991_g1), ACTB (Hs99999903_m1). Fluorescent emission was recorded in real-time using the ABI PRISM Sequence Detection System 7900HT (Applied Biosystems). PCR amplification conditions consisted of 45 cycles with primers annealing at 60 °C. Relative RNA quantities were normalized to the reference genes GAPDH and ACTB and untreated cells were used as a calibrating condition (ΔΔCt Method).

2.6. Statistical analysis

Statistical significance was assessed by one-way ANOVA with Dunnett's Multiple Comparison Test as Post Test, comparing all columns vs control (Ctr) column using the GraphPad Prism 5 software (<http://www.graphpad.com/>). All data represent the average of at least $n = 3$ biological replicates ± standard error mean (S.E.M.). For all graphs, an asterisk over a bar indicates a significant difference with the control group, an asterisk over a bracket shows a significant difference as indicated. For all graphs, * $p < 0.05$, ** $p < 0.01$, *** $p < 0.001$.

3. Results

3.1. Differentiation of hiPSCs into mixed neuronal/glial cultures

IMR90-hiPSCs were directly differentiated into mixed cultures of neuronal and glial cells for 28 days (Fig. 1A, part 1). In parallel, a protocol for rosette-derived neural stem cell (NSC) expansion and cryopreservation was developed as summarized in Fig. 1A (part 2). NSCs could be further differentiated into neurons and glial cells for 21 days (Fig. 1A, part 2).

Differentiated neuronal-like cells (28 days of differentiation) derived from IMR90-hiPSCs expressed high level of the major neuronal cytoskeleton protein, neurofilament 200 (NF200, approximately 65% of cells) and about 25–30% of the cells were positive for the glial fibrillary acidic protein (GFAP), marker of astroglia (Fig. 1B, C). We have also detected positive cells for the late marker of dendrites, microtubule-associated protein 2 (MAP2), as well as the pre-synaptic vesicle protein synaptophysin (Fig. 1B,

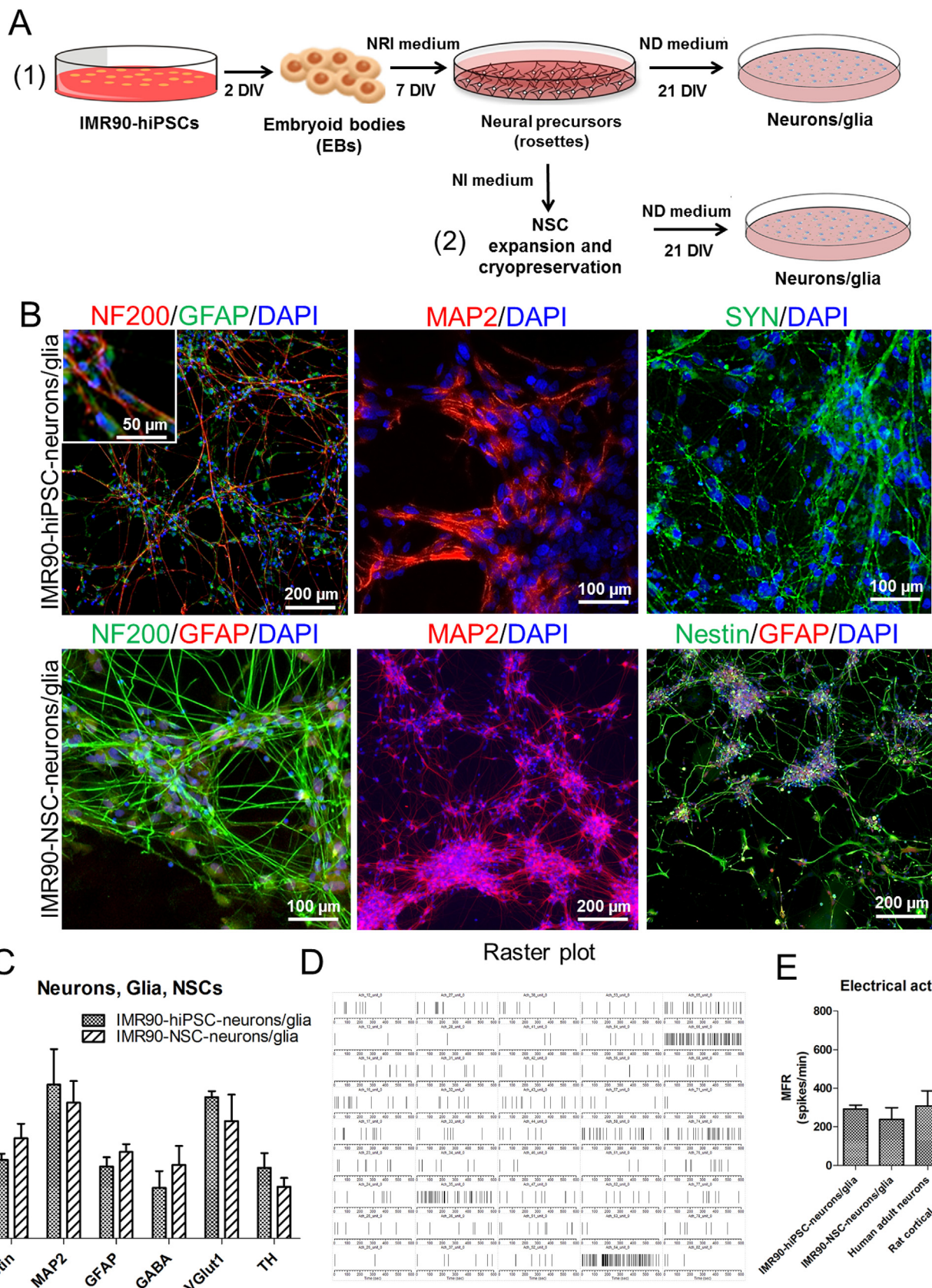


Fig. 1. Neuronal differentiation starting from IMR90-hiPSCs or from rosette-derived neural stem cells (NSCs) into mixed neuronal and glial cultures. (A) Schematic representation of the neural differentiation protocol: IMR90-hiPSC colonies were cut into fragments to form embryoid bodies (EBs). EBs were further cultured in the presence of neuroepithelial induction (NRI) medium to generate neuroectodermal derivatives (or rosettes), which were further differentiated into mature neuronal and glial cells in neuronal

upper panels). Similar results were obtained by analysing neuronal population obtained by expanding rosette-derived NSCs and their further differentiation into neurons (Fig. 1B, bottom panels). Moreover, in line with our previous report (Pistollato et al., 2014), we found that ~ 25–30% of cells still retained the expression of nestin after differentiation (Fig. 1B, C), and we observed no remarkable differences in the proportions of MAP2+, nestin+ and GFAP + cells between the two cell models (i.e., IMR90-hiPSC- vs IMR90-NSC-derivatives) (Fig. 1C).

Analysis of specific neuronal subpopulations in the two cultures models revealed that GABAergic neurons represented ~15–20%, dopaminergic neurons ~13–20%, and glutamatergic neurons ~35–42% of total cell number, as shown by analyses of immunocytochemistry for gamma-aminobutyric acid (GABA), tyrosine hydroxylase (TH) and Vesicular Glutamate Transporter 1 (VGluT1) respectively (Fig. 1C). The percentages of these cell subpopulations did not remarkably differ comparing differentiated cultures derived from IMR90-hiPSCs (Fig. 1A, part A) vs differentiated cells derived from IMR90-NSCs (Fig. 1A, part B).

Moreover, we assessed the spontaneous electrical activity of IMR90-derived neuronal-like cells. Rosette-derived NSCs (7 DIV) were plated on Multi Electrode Array (MEA) single-well chips (Multi Channel Systems) and further differentiated for 21 days (Fig. 1A). On day 28 of differentiation, neuronal spontaneous electrical activity was recorded, with a mean firing rate (MFR) of ~293 spikes/minute (Fig. 1E). Analogously, neurons derived from expanded NSCs yielded similar results with MFR of ~239 spikes/minute (Fig. 1D, E and Supplementary Fig. 1A, B). Additionally, we compared the MFR values of the hiPSC neuronal cultures with two different neuronal cell models: human neurons derived from adult brain tissue (Supplementary Fig. 1C) and rat embryonic cortical neurons, respectively cultured for 2 and 3 weeks on MEA chips to allow neuronal network maturation. Primary culture of rat neurons showed significantly higher electrical activity, with a MFR of ~730 spikes/min (Fig. 1E), presenting a massive generation of bursts as previously described (Vassallo et al., 2016). The MFR recorded from adult human neuronal cultures resulted in similar MFR value (~300 spikes/min) (Fig. 1E and Supplementary Fig. 1D) to the ones recorded for hiPSC-derived neurons. However, while human adult neurons generated also some bursts (Supplementary Fig. 1E), we could not observe bursts in hiPSC-neuronal cultures (data not shown).

3.2. Nuclear translocation of Nrf2 and upregulation of the antioxidant enzymes NQO1 and SRXN1 after exposure to different concentrations of rotenone

Rotenone has been shown to cause oxidative stress triggering the translocation of Nrf2 from the cytoplasm into the nucleus, followed by induction of the Nrf2-ARE target gene transcription (Tufekci et al. 2011). In order to assess the effects of rotenone, IMR90-derived neurons were exposed to 3 different concentrations of rotenone (1, 10 and 100 nM) for 24 h (Fig. 2A). These concentrations were established according to previous studies (Kovac et al., 2015; Lee et al., 2003). 1 nM concentration seems to be relevant to human exposure, as 0.55 ng/ml (~1 nM) was previously

found in the serum of a suicide-by-rotenone (Patel, 2011).

Analysis of total live cell numbers, by means of DAPI nuclear staining and high content imaging (HCl) (Fig. 2B) showed that rotenone at 1 and 10 nM was non-cytotoxic, however, 100 nM concentration caused a low level of cytotoxicity in IMR90-neurons (~15% cell death, not statistically significant). Additionally, we could not detect any significant change in the MFR value upon exposure to the three studied concentrations of rotenone (Fig. 2C and Supplementary Fig. 2), suggesting that rotenone at these concentrations and time of exposure (24 h) did not compromise spontaneous neuronal electrical activity.

Immunofluorescence analysis of Nrf2 protein showed an induction of Nrf2 nuclear translocation especially after exposing the cells to the highest concentration of rotenone (100 nM) (Fig. 2D, F). Furthermore, we assessed the expression of Keap1 (Kelch-like ECH-associated protein 1), a key post-induction repressor of Nrf2 (Bryan et al., 2013). After 24 h, cells exposed to rotenone, especially to the highest concentration (100 nM) showed a significant decrease of Keap1 protein levels in the cytoplasm (Fig. 2E), while Keap1 nuclear fraction did not change significantly (not shown).

Nrf2 is a key transcription factor involved in the activation of several genes that regulate antioxidant defence mechanisms. One of them is NQO1 (NAD(P)H quinone oxidoreductase 1) that has an important role in the quinone metabolism (Li et al., 2014; Tufekci et al., 2011), whereas SRXN1 (sulfiredoxin 1) catalyzes the reversal of overoxidation of peroxiredoxins and deglutathionylation induced by oxidative stress (Tufekci et al., 2011; Zhou et al., 2015). Immuncytochemical analysis of NQO1 and SRXN1 revealed a concentration-dependent increase of both protein levels upon exposure to 10 and 100 nM of rotenone (Fig. 2G). Conversely, analysis of NQO1, SRXN1 and GSR (glutathione reductase) expression, known Nrf2-target genes (Gorrini et al., 2013), did not show significant variations among the different rotenone concentrations (Fig. 2H) when compared to control levels, except for the Nrf2-target gene HMOX1 (heme oxygenase-1), where tendency towards higher expression was observed in a concentration-dependent manner (Fig. 2H).

Additionally, to confirm the role of Nrf2 signaling activation upon induction of oxidative stress, we treated hiPSC-derived neurons with 10 or 100 μM H₂O₂ (positive control) for 24 hr. These concentrations of H₂O₂ were comparable with those found in post-ischemia state, as reported in previous studies (Bell et al., 2011; Hyslop et al., 1995). At the highest concentration (100 μM) H₂O₂ elicited ~ 25% Nrf2 nuclear translocation (Supplementary Fig. 3A, D), while rotenone at the highest tested concentration (100 nM) promoted ~ 60% Nrf2 nuclear translocation, as reported above (Fig. 2D). Additionally, we found that H₂O₂ increased by ~70% the level of SRXN1 protein compared to control, whilst NQO1 and Keap1 protein levels did not change significantly (Supplementary Fig. 3B, C, E and F) in contrast to rotenone (Fig. 2E, G). These results suggest differences in cell response mechanisms activated upon exposure to either rotenone or H₂O₂.

Moreover, qPCR analyses of Nrf2 target genes (i.e., SRXN1, NQO1, HMOX1 and GSR) showed no significant differences between H₂O₂-treated vs untreated cells (Supplementary Fig. 3G). The absence of changes in the expression of Nrf2-target genes upon

differentiation (ND) medium (1). Rosette-derived neural stem cells (NSCs) could be expanded in the presence of neural induction (NI) medium or directly differentiated in the presence of ND medium to form mixed neuronal/glial cultures (2). (B) Representative immunocytochemical images of IMR90-hiPSC-derived neurons stained for neurofilament 200 (NF200: red), glial fibrillary acidic protein (GFAP: green), microtubule-associated protein-2 (MAP2: red) and synaptophysin (SYN: green) (upper panels), and IMR90-NSC-derived neurons stained for NF200 (green), GFAP (red), MAP2 (red) and nestin (green) (bottom panels). (C) Quantification of nestin, MAP2, GFAP, gamma-aminobutyric acid (GABA), vesicular glutamate transporter 1 (VGluT1) and tyrosine hydroxylase (TH) positive cells by HCl, using the Array Scan vTi platform, comparing IMR90-hiPSC-derivatives and derivatives obtained from expanded and cryopreserved IMR90-hiPSC derived NSCs. (D) Representative raster plot of IMR90-NSC-derived neurons obtained from 45 microelectrodes; recording was carried out for a minimum of 600 s, vertical bars represent single spikes. (E) Mean firing rate (MFR, number of spikes/minute) of IMR90-hiPSC-derived neurons, IMR90-NSC-derived neurons, human adult neurons, and rat embryonic cortical neurons.

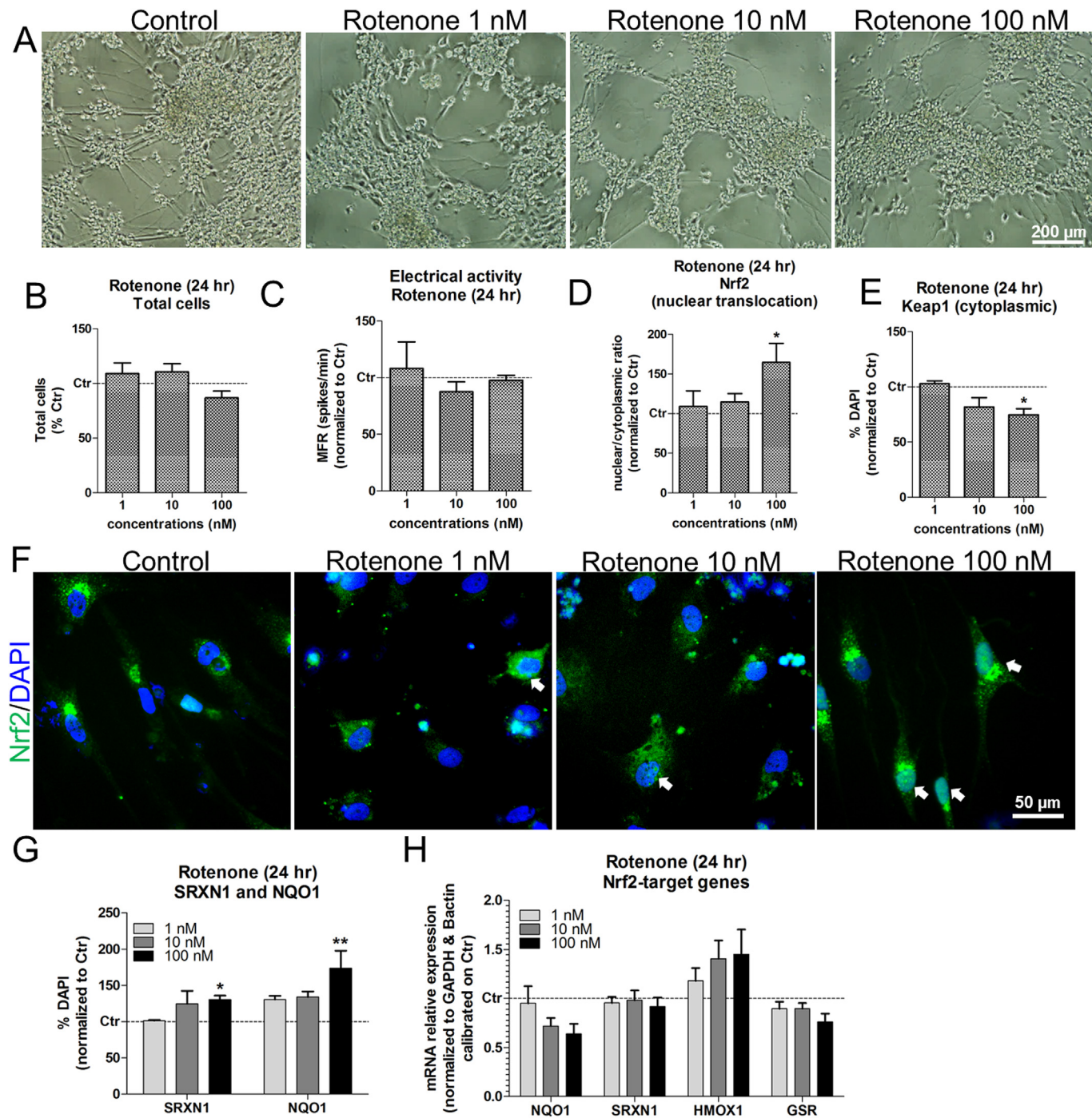


Fig. 2. Effects of rotenone on Nrf2 on nuclear translocation, Keap1 and antioxidant enzyme levels in IMR90-hiPSCs derived neurons. (A) Representative phase bright images on IMR90-hiPSC-derived neurons treated with 1, 10, 100 nM rotenone for 24 h. (B) Quantification of live DAPI⁺ cells (i.e. non-pyknotic nuclei), after exposure to different concentration of rotenone (1, 10, 100 nM) for 24 h and normalized to untreated, control cells (Ctr). (C) Values of MFR (number of spikes/min) of IMR90-hiPSC derived neurons after acute (24 h) exposure to 1–10–100 nM rotenone, normalized to untreated (Ctr) cells. (D) Quantification of Nrf2 protein nuclear translocation (i.e., nuclear: cytoplasmic signals ratios) in IMR90-hiPSC-derived neurons after 24 h of exposure to rotenone assessed by measurements of fluorescence intensity using HCl analysis. (E) Quantification of cytoplasmic Keap1 protein quantification assessed by HCl analysis, performed after exposure to rotenone for 24 h. (F) Representative immunocytochemical images of subcellular localization of Nrf2 (arrows indicate nuclear Nrf2 location). (G) Quantitative evaluation of NAD(P)H Quinone Oxidoreductase 1 (NQO1) and Sulfiredoxin1 (SRXN1) by means of immunocytochemistry and HCl after concentration-dependent treatment with rotenone for 24 h. (H) qPCR analyses of the Nrf2-target genes NQO1, SRXN1, HMOX1 (Heme Oxygenase-1) and GSR (Glutathione Reductase) (all values were normalized to β -actin and GAPDH (Glyceraldehyde 3-phosphate dehydrogenase) and then calibrated to untreated (Ctr) cells (dashed line) ($\Delta\Delta Ct$ method)). Values are shown as mean \pm S.E.M. of three biological replicates ($n = 3$) (* $p < 0.05$, ** $p < 0.01$).

treatment with H₂O₂ could be due to the fact that our hiPSC-derived mixed neuronal/glial model is particularly enriched in neurons (~70–75% of total cells), while astrocytes, which constitute ~25–30% of total cells, have been reported to be the sole

locus for Nrf2 activation by H₂O₂–mediated oxidative stress (Bell et al., 2011).

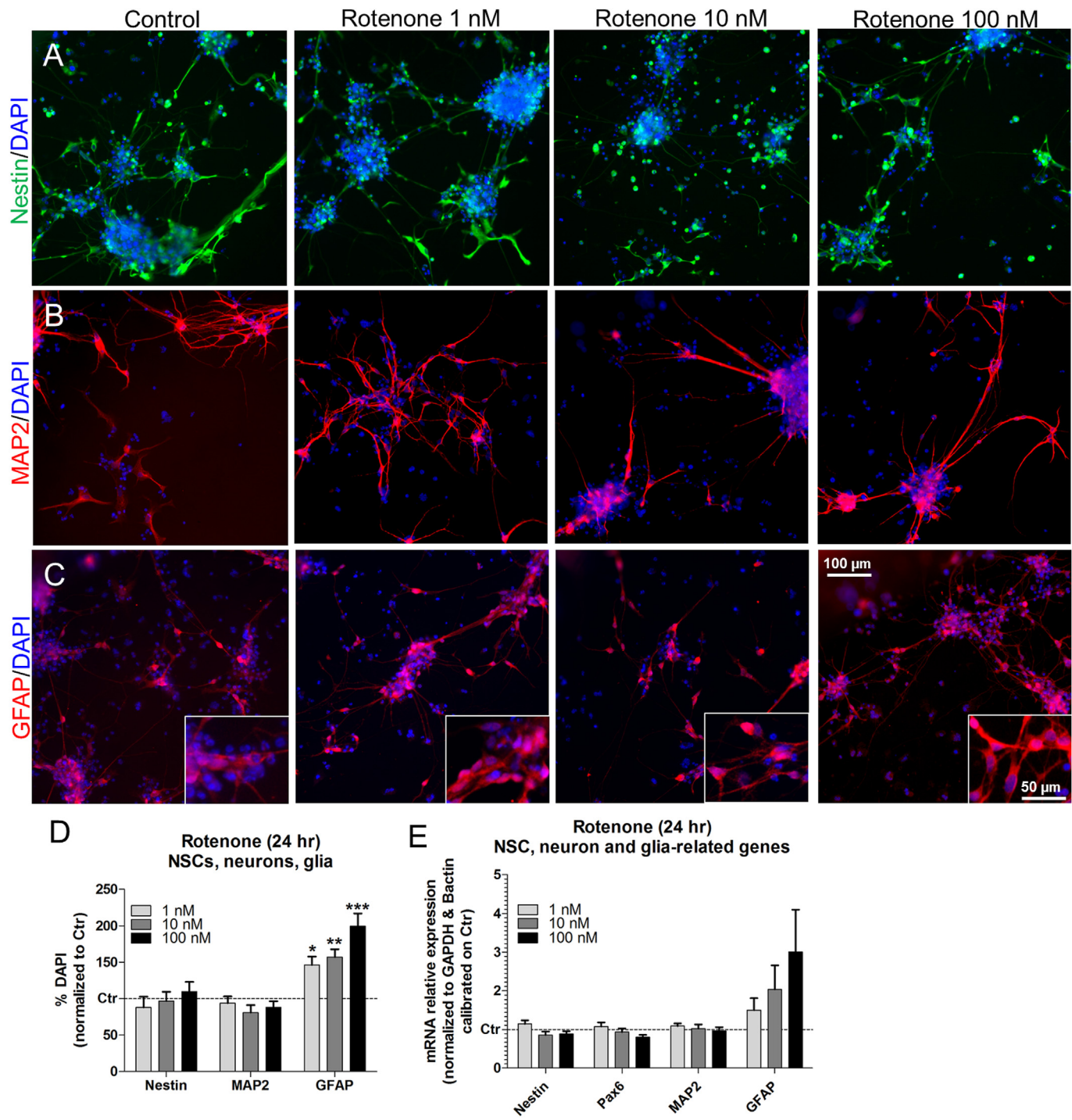


Fig. 3. Effects of rotenone on NSCs, neuronal and glial cells. (A–C) Representative immunocytochemical images of nestin (green, A), MAP2 (red, B) and GFAP (red, C, with 40X magnification insets) positive cells after exposure to different concentrations of rotenone (1 nM, 10 nM and 100 nM) for 24 h. (D) Quantitative evaluation of the three cell populations analyzed by HCl, using the Array Scan vTi platform, after exposure to rotenone. (E) qPCR analyses of Nestin, Pax6 (Paired Box 6), MAP2 and GFAP gene expression (all values were normalized to β -actin and GAPDH and then calibrated to Ctr cells (dashed line), $\Delta\Delta Ct$ method). All values are shown as mean \pm S.E.M. of three biological replicates ($n = 3$) (* $p < 0.05$, ** $p < 0.01$, *** $p < 0.001$).

3.3. Increase of astroglial cells in a concentration-dependent manner after exposure to rotenone

We further analyzed the percentage of nestin+ cells upon rotenone treatment compared to control group and we could not find significant differences among the tested conditions (Fig. 3A, D), suggesting that number of neural precursor cells did not

changed upon rotenone exposure. We also assessed the effects of rotenone on advanced neuronal cell differentiation, by analyzing the level of MAP2 protein via immunofluorescence and HCl, and we found that MAP2+ cell percentage did not change upon rotenone treatment (Fig. 3B, D). qPCR analyses of NSC specific genes (i.e., Nestin and Pax6) mainly confirmed the immunofluorescence and HCl data, showing that both Nestin and Pax6 did

not significantly change upon treatment with rotenone (Fig. 3E). Interestingly, rotenone induced a concentration-dependent increase of astroglial cells in the IMR90-derived mixed neuronal/glial cultures, promoting respectively a ~46%, ~57% and ~99%

increase in the number of GFAP+ cells compared to control (Fig. 3C, D), which was also confirmed by qPCR analysis of GFAP gene expression (Fig. 3E).

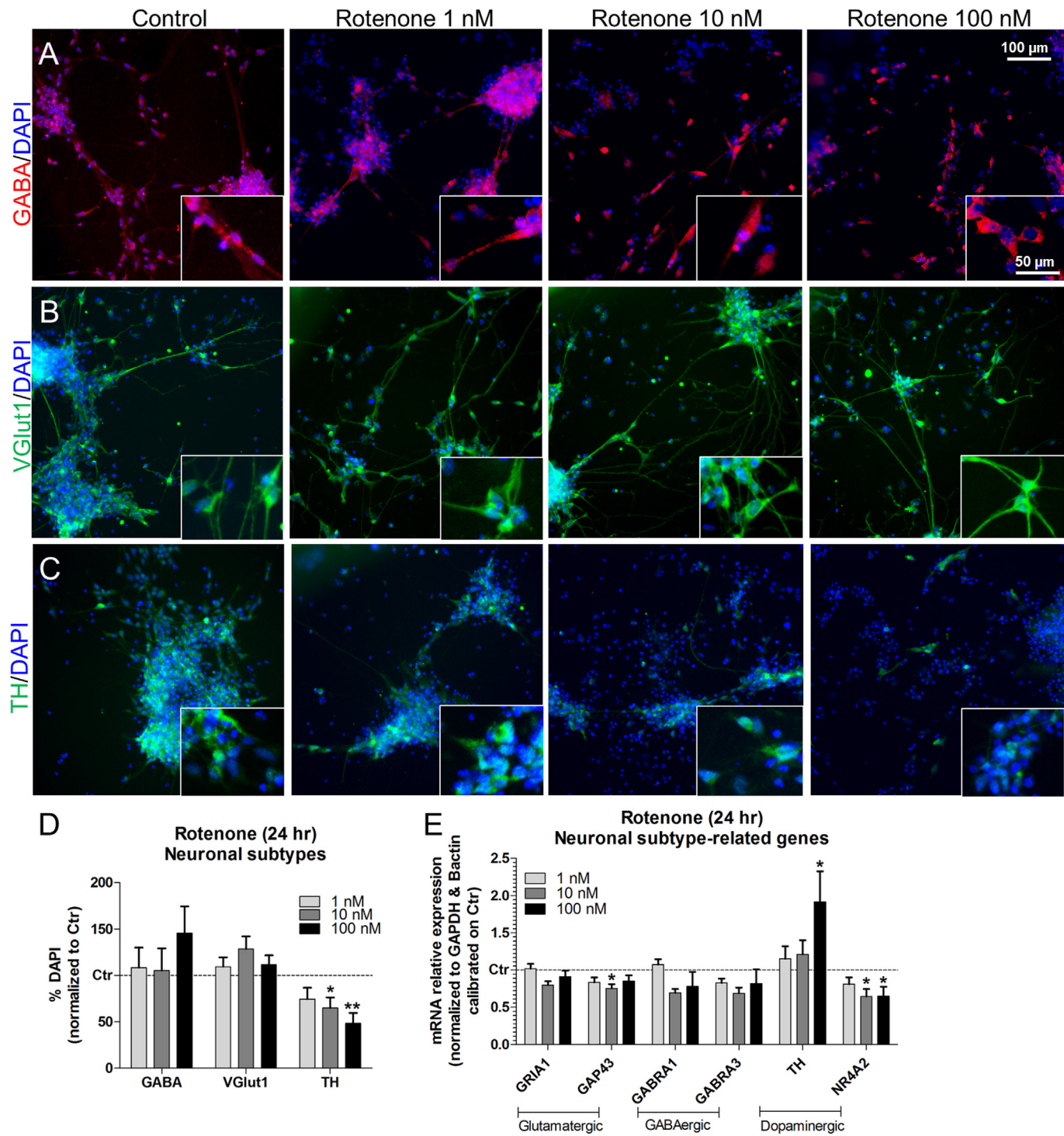


Fig. 4. Effects of rotenone on specific neuronal subpopulations. (A–C) Representative immunocytochemical images of GABA (red, A), VGluT1 (green, B) and TH (green, C) positive cells after exposure to different concentrations of rotenone (1 nM, 10 nM and 100 nM) for 24 h, with 40X magnification insets. (D) Quantification of the three cell populations analyzed by HCl, using the Array Scan vTi platform, after exposure to rotenone. (E) qPCR analyses of GRIA1 (Glutamate Ionotropic Receptor AMPA Type Subunit 1), GAP43 (Growth Associated Protein 43), GABRA1 (Gamma-Aminobutyric Acid Type A Receptor Alpha1 Subunit), GABRA3 (Gamma-Aminobutyric Acid Type A Receptor Alpha3 Subunit), TH (Tyrosine Hydroxylase), NR4A2 (Nuclear Receptor Subfamily 4 Group A Member 2), (all values were normalized to β -actin and GAPDH and then calibrated to Ctr cells (dashed line) ($\Delta\Delta Ct$ method)). All values are shown as mean \pm S.E.M. of three biological replicates ($n = 3$) (* $p < 0.05$, ** $p < 0.01$).

3.4. Rotenone treatment decreases the number of dopaminergic neurons

It has been previously shown that rotenone selectively elicits a dopaminergic neuronal cell death, as observed in *in vivo* (Cannon et al., 2009; Sherer et al., 2003) and *in vitro* studies (Testa et al., 2005). We investigated the effects elicited by a 24 h rotenone exposure on dopaminergic, GABAergic and glutamatergic neuronal markers. Immunofluorescence and HCl analysis revealed that the percentages of GABAergic and glutamatergic neurons did not significantly change upon rotenone treatment (Fig. 4A, B, D). However, GABA⁺ neurons appeared less elongated, especially at 100 nM rotenone (Fig. 4A, insets), which could be an indication of cellular stress. Importantly, TH⁺ cells were significantly decreased by rotenone treatment, especially at the highest tested concentration (i.e., 10 nM and 100 nM) (Fig. 4C, D).

We also analyzed the gene expression of some specific GABAergic (i.e., GABRA1 and GABRA3), glutamatergic (i.e., GRIA1 and GAP43) and dopaminergic (i.e., TH and NR4A2) neuronal-related genes. These analyses revealed no significant variations for GABRA1, GABRA3 and GRIA1, while the glutamatergic neuron-related gene GAP43 and, in particular, the dopaminergic gene NR4A2 (Nurr1) resulted significantly downregulated by rotenone (Fig. 4E). On the contrary, TH gene expression, opposite to TH protein level (Fig. 4C, D), resulted significantly increased, especially at the highest tested concentration (100 nM, Fig. 4E).

4. Discussion

The current study describes the concentration-dependent effects of rotenone on the Nrf2 pathway activation in hiPSC-derived mixed neuronal/glial cultures. HiPSCs- or NSCs-derived neuronal/glial mixed cultures are considered as promising models for *in vitro* neurotoxicity testing, since these neurons can reach advanced stage of morphological and functional differentiation (Bal-Price et al., 2010; Hou et al., 2013; Wheeler et al., 2015). Additionally, hiPSCs can be used for personalized toxicological risk assessment and thus support the prediction of individual susceptibility to specific environmental compounds (Kumar et al., 2012).

In the present study we have used a previously established protocol for the differentiation of hiPSCs into mixed neuronal and glial cell population (Pistollato et al., 2014). The differentiated cultures were composed of both neurons expressing classical neuronal marker proteins, such as NF200 and MAP2, synaptophysin and GFAP⁺ astrocytes. The presence of astrocytes is important since they play a fundamental role in neuronal homeostasis (oxidative stress defence mechanisms, extracellular glutamate uptake, ions balance, etc.) and function of neuronal networks (Barker and Ullian, 2008; Bell et al., 2011; Figley and Stroman, 2011; Santello and Volterra, 2009). Additionally, in line with our previous report (Pistollato et al., 2014), different neuronal subtypes, such as GABAergic, glutamatergic and dopaminergic neurons were identified. The functional maturation of derived neurons was studied by analysing their electrical activity (MFR) using multi-electrode arrays that is nowadays one of the most reliable tools for neuronal function evaluation (Odawara et al., 2014). The obtained results suggest that functional neuronal network was created, however a lack of synchronized bursting indicates that these neurons did not reach terminal functional maturation, as it was observed in primary cultures of rat embryonic cortical neurons.

In parallel, we developed a protocol for the expansion of rosette-derived NSCs, their cryopreservation and further differentiation into neuronal cells. Differentiation of neurons from NSCs should reduce variability and improve reproducibility of the obtained results. In our studies the proportion of obtained neurons and their

electrical activity measured by MFR resulted similar, irrespectively whether the neurons were differentiated directly from hiPSCs or from NSCs. Considering the presence of ~25–30% of astrocytes in this mixed neuronal/glial culture, further analyses should be done to assess whether astrocytes in this mixed hiPSC neuronal/glial model can contribute to the calcium waves propagation observed during the generation of neuronal electrical activity. Indeed, Tamura and colleagues have observed a metabotropic glutamate receptor 5 (mGluR5)-dependent spontaneous slow Ca²⁺ oscillation in both neurons and astrocytes in the striatum of murine brain slices (Tamura et al., 2014).

Several neurodegenerative diseases are characterized by mitochondrial dysfunction and increased oxidative stress (Nicholls and Budd, 2000; Tufekci et al., 2011), which may result upon exposure to neurotoxicants. Oxidative stress is one of the early effects observed in neuronal cultures exposed to different classes of chemicals, including inhibitors of mitochondrial respiration chain such as rotenone (Peng et al., 2013). In an effort to restore homeostasis, neuronal cells respond to these chemical entities by activating signaling pathways, such as the Nrf2/ARE, which is known to play a cytoprotective, antioxidant and anti-inflammatory role (Lee et al., 2003; Shih et al., 2005; Tufekci et al., 2011). Under physiological conditions the protein levels of Nrf2 are kept low in the cytoplasm due to the rapid proteasome-mediated turnover facilitated by the Keap1 protein, which acts as a Nrf2-specific ligase adaptor protein (Gorrini et al., 2013; Hartikainen et al., 2012; Harvey et al., 2009; Kansanen et al., 2013). In response to various extracellular signals triggering oxidative stress the inhibitory effects of Keap1 on Nrf2 is interrupted, Nrf2 dissociates from Keap1 resulting in translocation and accumulation in the nucleus (Kovac et al., 2015; Tufekci et al., 2011). Therefore in the present study we have evaluated both Nrf2 and Keap1 expression upon an exposure to rotenone (positive control) that is known to induce ROS production upon inhibition of complex I of mitochondrial respiratory chain (Satoh et al., 2009).

Here, we show that a concentration-dependent exposure to rotenone for 24 h caused an activation of Nrf2 pathway causing Nrf2 nuclear translocation, as shown by immunocytochemical analysis and HCl of Nrf2 protein levels. In parallel, we found that rotenone elicited a significant decrease of cytoplasmic Keap1 protein.

Recent studies suggest that Keap1 has a dual role in maintaining cellular homeostasis after exposure to chemicals, by providing dependent and independent regulation of the Nrf2 pathway (Bryan et al., 2013). Previous observations have revealed that upon oxidative stress, Keap1 exhibits a conformational change that results in the release of Nrf2 and its trafficking and accumulation into the nucleus, in order to bind to gene promoter regions containing ARE (Harder et al., 2015; Lee et al., 2003; Ramsey et al., 2007). Notwithstanding, recent publications also support the idea that Keap1 could be involved in a post-induction repressor of Nrf2 signaling, due to its ability to independently enter into the nucleus, dissociate Nrf2 from ARE, and transfer Nrf2 back to the cytoplasm (Bryan et al., 2013; Satoh et al., 2009; Sun et al., 2007). As both Keap1-dependent and independent mechanisms of regulation of the Nrf2 pathway have been described (Bryan et al., 2013) further studies are needed to clarify the significance of our data, showing a reduction of cytoplasmic Keap1 levels upon rotenone treatment (Fig. 2E).

Nrf2 plays a pivotal role in the transcription of several ARE-dependent cytoprotective genes including NQO1 and SRXN1 (Itoh et al., 1997; Li et al., 2014) that were evaluated in this study after exposure to rotenone at different concentrations (1, 10 and 100 nM). While qPCR analysis did not reveal significant variations of gene expression, apart from a modest upregulation of HMOX1

gene expression, both NQO1 and SRXN1 protein levels were increased in a concentration-dependent manner upon treatment with rotenone, which confirms activation of the Nrf2 pathway (Li et al., 2014). Presumably, rotenone-induced inhibition of complex I triggered ROS production, followed by Nrf2 pathway activation (Barrientos and Moraes, 1999). Increased ROS production causes oxidative damage to DNA, lipids and proteins, and up regulation of NQO1 and SRXN1 protects cells against these effects. NQO1 catalyzes the reduction of highly reactive quinones that can cause redox cycling and oxidative stress, while SRXN1 reduces cysteine-sulfenic acid formed under exposure to oxidants in the peroxiredoxins PRDX1, PRDX2, PRDX3 and PRDX4 (Ma, 2013). Additionally, Nrf2 directly affects homeostasis of ROS by catabolism of superoxide and peroxides, regeneration of oxidized cofactors and proteins, synthesis of reducing factors (i.e., reduced glutathione by glutamate-cysteine ligase catalytic subunit, etc.) (Ma, 2013). Although the list of Nrf2 target genes varies depending on cell type, Nrf2 is critical to the cellular defense mechanisms in many tissues, including the brain (Lee et al., 2003; Shih et al., 2005).

In the same study, we also detected a concentration-dependent increase of GFAP gene expression and protein level (by immunocytochemistry), after exposure to rotenone, which could indicate astrocyte activation (Bal-Price et al., 2010; Cabezas et al., 2012; Swarnkar et al., 2012). It is well known that astrocytes respond to different neurological insults, such as oxidative stress, by reactive astrogliosis, which involves the increase of astrocytes, molecular and conformational changes of the cells, and GFAP up-regulation, which is controlled by different cytokines and neurohormones (Radad et al., 2008; Swarnkar et al., 2012). Astrocyte-specific Nrf2 target genes play an important role in antioxidant and anti-inflammatory effects in brain. Recently it was reported that Nrf2 regulates the synthesis and release of reduced glutathione (GSH) by astrocytes (Steele et al., 2013). Another study suggests that neuro-protective effect of Nrf2 involves genetic remodeling (i.e., ARE-driven gene expression) of both astrocytes and neurons (Lee et al., 2003). Indeed, Nrf2-knockout mice were significantly more sensitive to mitochondrial complex I and II inhibitors and transplanted Nrf2-overexpressing astrocytes into the mouse striatum, prior to lesioning with malonate, led to dramatic protection against neurotoxicity, suggesting that astrocytes are central to Nrf2-ARE mediated neuroprotection (Johnson et al., 2008).

Opposite to Pei's study (Pei et al., 2016) we did not observe significant variations in the percentages of both nestin⁺ and MAP2⁺ cells. It should also be considered that the concentrations tested in our study are about 10³ times lower than the ones tested in Pei's experiments (i.e., 1 and 10 μM respectively) (Pei et al., 2016), which could contribute to the differences in rotenone effects observed in our study.

Decreased number of TH⁺ cells induced by rotenone (Fig. 4C, D), is in line with previous studies showing a selective dopaminergic neuronal cell death caused by rotenone *in vitro* (Testa et al., 2005) and *in vivo* (Cannon et al., 2009; Sherer et al., 2003). Dopaminergic neurons are the most vulnerable population of neurons to various stressors, including oxidative stress (Fujita et al., 2014). Interestingly, rotenone was also reported to upregulate TH mRNA, as described in PC12 cells cultured at 20% oxygen (Hohler et al., 1999). The observed increase of TH gene expression particularly at the highest tested rotenone concentration (100 nM, Fig. 4E) could be possibly associated with compensatory mechanisms induced in the surviving cells to recover the reduction of TH protein elicited by the acute exposure to rotenone.

Moreover, acute treatment with rotenone did not elicit significant changes in electrical activity of hiPSC-derived cultures (Fig. 2C and Supplementary Fig. 2) when compared to the control cultures. On the contrary, Gao and co-workers have shown that rotenone at 1

and 3 μM can decrease the delayed rectifier K⁺ current (I_{DR}) amplitude, whilst not having effect on A-type current (I_A) peak amplitude (Gao et al., 2008). However, possible extrapolations of these data might be challenging, considering that Gao's study was conducted on cultured ventral mesencephalic rodent neurons (rather than hiPSC-derived neurons), using whole-cell patch clamp (rather than multi-electrode array).

In conclusion, the obtained data indicate that hiPSC-derived mixed neuronal/glial culture could be a valuable tool for studying the neurotoxic effects of chemicals that induce oxidative stress, particularly if Nrf2 pathway becomes activated. However, it will be important to assess Nrf2 activation across different classes of chemicals, in order to identify which specific genes/proteins are up- or down-regulated in order to be used as potential biomarkers of Nrf2 signaling pathway activation. Oxidative stress is an important and common key event in various Adverse Outcome Pathways (AOPs) relevant to developmental and adult neurotoxicity (Bal-Price et al., 2015b). The defined AOP key events, including Nrf2 pathway activation, could serve as a base for assay development needed to build integrated testing strategies (Bal-Price et al., 2015a), such as AOP-informed IATA (Integrated Approaches to Testing and Assessment) for neurotoxicity testing (Tollefsen et al., 2014), providing mechanistic knowledge to facilitate regulatory decision making process.

5. Conclusions

The obtained data suggest that mixed, neuronal/glial culture derived from hiPSCs could serve as a promising model for *in vitro* neurotoxicity testing of chemicals that induce oxidative stress and trigger Nrf2 pathway activation. Moreover, NQO1 and SRXN1, specific Nrf2-target genes, could be possibly recognized as biomarkers of chemically induced oxidative stress.

Funding

This work was supported by the EU-funded project "SCR&Tox" (Grant Agreement N°. 266753).

Declaration of interests

The authors have no conflict of interest to declare.

Acknowledgments

The authors would like to thank Dr. Giovanna Lazzari and Dr. Silvia Colleoni (Avantea srl, Cremona, Italy), Dr. Simone Haupt (University of Bonn, Germany), Dr. Vania Rosas (Institute Pasteur, Paris, France) for fruitful discussions, Dr. Marc Peschanski (I-Stem, Évry, France) for providing IMR90-hiPSCs, Dr. Elisabeth Joossens (IHCP, JRC, Ispra, Italy) for statistical analyses, and Dr. Tiziana Santini (Italian Institute of Technology, Rome) for providing advice on immunofluorescence staining evaluation.

Appendix A. Supplementary data

Supplementary data related to this article can be found at <http://dx.doi.org/10.1016/j.neuint.2016.09.004>.

References

- Aviñor, Y., Sagi, I., Benvenisty, N., 2016 Mar. Pluripotent stem cells in disease modelling and drug discovery. *Nat. Rev. Mol. Cell Biol.* 17 (3), 170–182.
- Bal-Price, A., Crofton, K.M., Leist, M., Allen, S., Arand, M., Buetler, T., Delrue, N., FitzGerald, R.E., Hartung, T., Heinonen, T., Hogberg, H., Bennekou, S.H., Lichtensteiger, W., Oggier, D., Paparella, M., Axelstad, M., Piersma, A., Rached, E.,

- Schilter, B., Schmuck, G., Stoppini, L., Tongiorgi, E., Tiramani, M., Monnet-Tschudi, F., Wilks, M.F., Ylikomi, T., Fritzsche, E., 2015a. International STakeholder NETwork (ISTNET): creating a developmental neurotoxicity (DNT) testing road map for regulatory purposes. *Arch. Toxicol.* 89, 269–287.
- Bal-Price, A., Crofton, K.M., Sachana, M., Shafer, T.J., Behl, M., Forsby, A., Hargreaves, A., Landesmann, B., Lein, P.J., Louisse, J., Monnet-Tschudi, F., Paini, A., Rolaki, A., Schrattenholz, A., Sunol, C., van Thriel, C., Whelan, M., Fritzsche, E., 2015b. Putative adverse outcome pathways relevant to neurotoxicity. *Crit. Rev. Toxicol.* 45, 83–91.
- Bal-Price, A.K., Hogberg, H.T., Buzanska, L., Coecke, S., 2010. Relevance of in vitro neurotoxicity testing for regulatory requirements: challenges to be considered. *Neurotoxicol Teratol.* 32, 36–41.
- Barker, A.J., Ullian, E.M., 2008. New roles for astrocytes in developing synaptic circuits. *Commun. Integr. Biol.* 1, 207–211.
- Barrientos, A., Moraes, C.T., 1999. Titrating the effects of mitochondrial complex I impairment in the cell physiology. *J. Biol. Chem.* 274, 16188–16197.
- Bell, K.F., Al-Mubarak, B., Fowler, J.H., Baxter, P.S., Gupta, K., Tsujita, T., Chowdhry, S., Patani, R., Chandran, S., Horsburgh, K., Hayes, J.D., Hardingham, G.E., 2011. Mild oxidative stress activates Nrf2 in astrocytes, which contributes to neuroprotective ischemic preconditioning. *Proc. Natl. Acad. Sci. U. S. A.* 108, E1–E2; author reply E3–E4.
- Bryan, H.K., Olayanju, A., Goldring, C.E., Park, B.K., 2013. The Nrf2 cell defence pathway: keap1-dependent and -independent mechanisms of regulation. *Biochem. Pharmacol.* 85, 705–717.
- Cabezas, R., El-Bacha, R.S., Gonzalez, J., Barreto, G.E., 2012. Mitochondrial functions in astrocytes: neuroprotective implications from oxidative damage by rotenone. *Neurosci. Res.* 74, 80–90.
- Cannon, J.R., Tapias, V., Na, H.M., Honick, A.S., Drolet, R.E., Greenamyre, J.T., 2009. A highly reproducible rotenone model of Parkinson's disease. *Neurobiol. Dis.* 34, 279–290.
- Desbordes, S.C., Studer, L., 2013. Adapting human pluripotent stem cells to high-throughput and high-content screening. *Nat. Protoc.* 8, 111–130.
- Figley, C.R., Stroman, P.W., 2011. The role(s) of astrocytes and astrocyte activity in neurometabolism, neurovascular coupling, and the production of functional neuroimaging signals. *Eur. J. Neurosci.* 33, 577–588.
- Fujita, K.A., Ostaszewski, M., Matsuoka, Y., Ghosh, S., Glaab, E., Trefois, C., Crespo, I., Perumal, T.M., Jurkowski, W., Antony, P.M., Diederich, N., Buttini, M., Kodama, A., Satagopam, V.P., Eifes, S., Del Sol, A., Schneider, R., Kitano, H., Balling, R., 2014. Integrating pathways of Parkinson's disease in a molecular interaction map. *Mol. Neurobiol.* 49, 88–102.
- Gao, X.F., Wang, W., He, C., 2008. Rotenone inhibits delayed rectifier K⁺ current via a protein kinase A-dependent mechanism. *Neuroreport* 19, 1401–1405.
- Gorrini, C., Harris, I.S., Mak, T.W., 2013. Modulation of oxidative stress as an anti-cancer strategy. *Nat. Rev. Drug Discov.* 12, 931–947.
- Harder, B., Jiang, T., Wu, T., Tao, S., de la Vega, M.R., Tian, W., Chapman, E., Zhang, D.D., 2015. Molecular mechanisms of Nrf2 regulation and how these influence chemical modulation for disease intervention. *Biochem. Soc. Trans.* 43, 680–686.
- Hartikainen, J.M., Tengstrom, M., Kosma, V.M., Kinnula, V.L., Mannermaa, A., Soini, Y., 2012. Genetic polymorphisms and protein expression of NRF2 and Sulfiredoxin predict survival outcomes in breast cancer. *Cancer Res.* 72, 5537–5546.
- Harvey, C.J., Thimmappappa, R.K., Singh, A., Blake, D.J., Ling, G., Wakabayashi, N., Fujii, J., Myers, A., Biswal, S., 2009. Nrf2-regulated glutathione recycling independent of biosynthesis is critical for cell survival during oxidative stress. *Free Radic. Biol. Med.* 46, 443–453.
- Hohler, B., Lange, B., Holzapfel, B., Goldenberg, A., Hanze, J., Sell, A., Testan, H., Moller, W., Kummer, W., 1999. Hypoxic upregulation of tyrosine hydroxylase gene expression is paralleled, but not induced, by increased generation of reactive oxygen species in PC12 cells. *FEBS Lett.* 457, 53–56.
- Hou, Z., Zhang, J., Schwartz, M.P., Stewart, R., Page, C.D., Murphy, W.L., Thomson, J.A., 2013. A human pluripotent stem cell platform for assessing developmental neural toxicity screening. *Stem Cell Res. Ther.* 4 (Suppl. 1), S12.
- Hyslop, P.A., Zhang, Z., Pearson, D.V., Phuebs, L.A., 1995. Measurement of striatal H₂O₂ by microdialysis following global forebrain ischemia and reperfusion in the rat: correlation with the cytotoxic potential of H₂O₂ in vitro. *Brain Res.* 671, 181–186.
- Itoh, K., Chiba, T., Takahashi, S., Ishii, T., Igarashi, K., Katoh, Y., Oyake, T., Hayashi, N., Satoh, K., Hatayama, I., Yamamoto, M., Nabeshima, Y., 1997. An Nrf2/small Maf heterodimer mediates the induction of phase II detoxifying enzyme genes through antioxidant response elements. *Biochem. Biophys. Res. Commun.* 236, 313–322.
- Johnson, J.A., Johnson, D.A., Kraft, A.D., Calkins, M.J., Jakel, R.J., Vargas, M.R., Chen, P.C., 2008. The Nrf2-ARE pathway: an indicator and modulator of oxidative stress in neurodegeneration. *Ann. N. Y. Acad. Sci.* 1147, 61–69.
- Kansanen, E., Kuosmanen, S.M., Leinonen, H., Levonen, A.L., 2013. The Keap1-Nrf2 pathway: mechanisms of activation and dysregulation in cancer. *Redox Biol.* 1, 45–49.
- Kovac, S., Angelova, P.R., Holmstrom, K.M., Zhang, Y., Dinkova-Kostova, A.T., Abramov, A.Y., 2015. Nrf2 regulates ROS production by mitochondria and NADPH oxidase. *Biochim. Biophys. Acta* 1850, 794–801.
- Krueger, W.H., Swanson, L.C., Tanasijevic, B., Rasmussen, T.P., 2010. Natural and artificial routes to pluripotency. *Int. J. Dev. Biol.* 54, 1545–1564.
- Kumar, K.K., Aboud, A.A., Bowman, A.B., 2012. The potential of induced pluripotent stem cells as a translational model for neurotoxicological risk. *Neurotoxicology* 33, 518–529.
- Lee, J.M., Shih, A.Y., Murphy, T.H., Johnson, J.A., 2003. NF-E2-related factor-2 mediates neuroprotection against mitochondrial complex I inhibitors and increased concentrations of intracellular calcium in primary cortical neurons. *J. Biol. Chem.* 278, 37948–37956.
- Li, L., Dong, H., Song, E., Xu, X., Liu, L., Song, Y., 2014. Nrf2/ARE pathway activation, HO-1 and NQO1 induction by polychlorinated biphenyl quinone is associated with reactive oxygen species and PI3K/AKT signaling. *Chem. Biol. Interact.* 209, 56–67.
- Ma, Q., 2013. Role of nrf2 in oxidative stress and toxicity. *Annu. Rev. Pharmacol. Toxicol.* 53, 401–426.
- Nicholls, D.G., Budd, S.L., 2000. Mitochondria and neuronal survival. *Physiol. Rev.* 80, 315–360.
- NRC, 2007. *Toxicity Testing in the 21st Century: a Vision and a Strategy*. National Academy Press, Washington (DC). <http://dx.doi.org/10.17226/11970>. ISBN: 978-0-309-15173-3.
- O'Brien, P.J., Irwin, W., Diaz, D., Howard-Cofield, E., Krejsa, C.M., Slaughter, M.R., Gao, B., Kaludercic, N., Angeline, A., Bernardi, P., Brain, P., Hougham, C., 2006. High concordance of drug-induced human hepatotoxicity with in vitro cytotoxicity measured in a novel cell-based model using high content screening. *Arch. Toxicol.* 80, 580–604.
- Odawara, A., Saitoh, Y., Alhebshi, A.H., Gotoh, M., Suzuki, I., 2014. Long-term electrophysiological activity and pharmacological response of a human induced pluripotent stem cell-derived neuron and astrocyte co-culture. *Biochem. Biophys. Res. Commun.* 443, 1176–1181.
- Patel, F., 2011. Pesticidal suicide: adult fatal rotenone poisoning. *J. Forensic Leg. Med.* 18, 340–342.
- Pei, Y., Peng, J., Behl, M., Sipes, N.S., Shockley, K.R., Rao, M.S., Tice, R.R., Zeng, X., 2016. Comparative neurotoxicity screening in human iPSC-derived neural stem cells, neurons and astrocytes. *Brain Res.* 1638, 57–73.
- Peng, J., Liu, Q., Rao, M.S., Zeng, X., 2013. Using human pluripotent stem cell-derived dopaminergic neurons to evaluate candidate Parkinson's disease therapeutic agents in MPP+ and rotenone models. *J. Biomol. Screen* 18, 522–533.
- Pistollato, F., Bremer-Hoffmann, S., Healy, L., Young, L., Stacey, G., 2012. Standardization of pluripotent stem cell cultures for toxicity testing. *Expert Opin. Drug Metab. Toxicol.* 8, 239–257.
- Pistollato, F., Louisse, J., Scelfo, B., Mennecozzi, M., Accordi, B., Basso, G., Gaspar, J.A., Zagoura, D., Barilaro, M., Palosaari, T., Sachinidis, A., Bremer-Hoffmann, S., 2014. Development of a pluripotent stem cell derived neuronal model to identify chemically induced pathway perturbations in relation to neurotoxicity: effects of CREB pathway inhibition. *Toxicol. Appl. Pharmacol.* 280, 378–388.
- Radad, K., Gille, G., Rausch, W.D., 2008. Dopaminergic neurons are preferentially sensitive to long-term rotenone toxicity in primary cell culture. *Toxicol. In Vitro* 22, 68–74.
- Ramsey, C.P., Glass, C.A., Montgomery, M.B., Lindl, K.A., Ritson, G.P., Chia, L.A., Hamilton, R.L., Chu, C.T., Jordan-Sciutto, K.L., 2007. Expression of Nrf2 in neurodegenerative diseases. *J. Neuropathol. Exp. Neurol.* 66, 75–85.
- Robinton, D.A., Daley, G.Q., 2012. The promise of induced pluripotent stem cells in research and therapy. *Nature* 481, 295–305.
- Santello, M., Volterra, A., 2009. Synaptic modulation by astrocytes via Ca²⁺-dependent glutamate release. *Neuroscience* 158, 253–259.
- Satoh, T., Harada, N., Hosoya, T., Tohyama, K., Yamamoto, M., Itoh, K., 2009. Keap1/Nrf2 system regulates neuronal survival as revealed through study of keap1 gene-knockout mice. *Biochem. Biophys. Res. Commun.* 380, 298–302.
- Sherer, T.B., Kim, J.H., Betarbet, R., Greenamyre, J.T., 2003. Subcutaneous rotenone exposure causes highly selective dopaminergic degeneration and alpha-synuclein aggregation. *Exp. Neurol.* 179, 9–16.
- Shih, A.Y., Imbeault, S., Barakauskas, V., Erb, H., Jiang, L., Li, P., Murphy, T.H., 2005. Induction of the Nrf2-driven antioxidant response confers neuroprotection during mitochondrial stress in vivo. *J. Biol. Chem.* 280, 22925–22936.
- Steele, M.L., Fuller, S., Patel, M., Kersaitis, C., Ooi, L., Munch, G., 2013. Effect of Nrf2 activators on release of glutathione, cysteinylglycine and homocysteine by human U373 astroglial cells. *Redox Biol.* 1, 441–445.
- Sun, Z., Zhang, S., Chan, J.Y., Zhang, D.D., 2007. Keap1 controls postinduction repression of the Nrf2-mediated antioxidant response by escorting nuclear export of Nrf2. *Mol. Cell Biol.* 27, 6334–6349.
- Swarnkar, S., Singh, S., Goswami, P., Mathur, R., Patro, I.K., Nath, C., 2012. Astrocyte activation: a key step in rotenone induced cytotoxicity and DNA damage. *Neurochem. Res.* 37, 2178–2189.
- Tamura, A., Yamada, N., Yaguchi, Y., Machida, Y., Mori, I., Osanai, M., 2014. Both neurons and astrocytes exhibited tetrodotoxin-resistant metabotropic glutamate receptor-dependent spontaneous slow Ca²⁺ oscillations in striatum. *PLoS One* 9, e85351.
- Tanner, C.M., Kamel, F., Ross, G.W., Hoppin, J.A., Goldman, S.M., Korell, M., Marras, C., Bhudhikanok, G.S., Kasten, M., Chade, A.R., Comyns, K., Richards, M.B., Meng, C., Priestley, B., Fernandez, H.H., Cambi, F., Umbach, D.M., Blair, A., Sandler, D.P., Langston, J.W., 2011. Rotenone, paraquat, and Parkinson's disease. *Environ. Health Perspect.* 119, 866–872.
- Testa, C.M., Sherer, T.B., Greenamyre, J.T., 2005. Rotenone induces oxidative stress and dopaminergic neuron damage in organotypic substantia nigra cultures. *Brain Res. Mol. Brain Res.* 134, 109–118.
- Tollefson, K.E., Scholz, S., Cronin, M.T., Edwards, S.W., de Knecht, J., Crofton, K., Garcia-Reyero, N., Hartung, T., Worth, A., Patlewicz, G., 2014. Applying adverse outcome pathways (AOPs) to support integrated approaches to testing and assessment (IATA). *Regul. Toxicol. Pharmacol.* 70, 629–640.

- Tufekci, K.U., Civi Bayin, E., Genc, S., Genc, K., 2011. The Nrf2/are pathway: a promising target to counteract mitochondrial dysfunction in Parkinson's disease. *Park. Dis.* 2011, 314082.
- Vassallo, A., Chiappalone, M., De Camargos Lopes, R., Scelfo, B., Novellino, A., Defranchi, E., Palosaari, T., Weisschu, T., Ramirez, T., Martinoia, S., Johnstone, A.F., Mack, C.M., Landsiedel, R., Whelan, M., Bal-Price, A., Shafer, T.J., 2016. A multi-laboratory evaluation of microelectrode array-based measurements of neural network activity for acute neurotoxicity testing. *Neurotoxicology*.
- Wheeler, H.E., Wing, C., Delaney, S.M., Komatsu, M., Dolan, M.E., 2015. Modeling chemotherapeutic neurotoxicity with human induced pluripotent stem cell-derived neuronal cells. *PLoS One* 10, e0118020.
- Yap, M.S., Nathan, K.R., Yeo, Y., Lim, L.W., Poh, C.L., Richards, M., Lim, W.L., Othman, I., Heng, B.C., 2015. Neural differentiation of human pluripotent stem cells for nontherapeutic applications: toxicology, pharmacology, and in vitro disease modeling. *Stem Cells Int.* 105172.
- Zhou, Y., Duan, S., Zhou, Y., Yu, S., Wu, J., Wu, X., Zhao, J., Zhao, Y., 2015. Sulfiredoxin-1 attenuates oxidative stress via Nrf2/ARE pathway and 2-Cys Prdxs after oxygen-glucose deprivation in astrocytes. *J. Mol. Neurosci.* 55, 941–950.